# Analytic Expression for the Ideal One-dimensional Mirror Potential Yielding Perfect Energy Focusing in TOF Mass Spectrometry

Curt A. Flory, Robert C. Taber, and George E. Yefchak
*Hewlett-Packard Laboratories, 3500 Deer Creek Road, Palo Alto, CA 94304 USA*

**Abstract**

The resolving power of a Wiley-McLaren time-of-flight mass spectrometer can be severely limited by the longitudinal velocity spread of ions originating from the same position along the flight path. This effect is normally minimized by using an electrostatic mirror to reflect the incident ions from their original direction back toward the spectrometer detector, in which case higher velocity ions have a greater delay time in the mirror due to their further penetration into the mirror potential, and spatial focusing occurs at the plane of the detector. In this paper, an analytic expression is obtained for the ideal one-dimensional mirror potential that yields perfect spatial focusing along the flight path. The mathematical techniques used are those commonly employed in the solution of calculus of variations problems.

## I. Introduction

The linear time-of-flight (TOF) mass spectrometer described by Wiley and McLaren [1] consists of an extraction region containing the initial distribution of ions to be separated, acceleration and field-free drift regions, and a detector. Ion packets are launched out of the extraction region by a suddenly applied voltage gradient. The accelerated packet of ions travels through the field-free drift region, and at a certain position along the flight path called the space-focus plane, the packet has a minimum spatial extent (or temporal spread). This spatial focusing occurs due to the fact that ions which were originally further away from the exit grid of the extraction region gain more energy during the extraction process than those initially close to the exit. Thus, as the packet of ions travels through the drift region, the trailing ions eventually will overtake the lower energy leading edge, producing a pulse of minimum width at the space-focus plane.

To achieve minimum isomass pulse width, the detector would normally be placed at the space-focus plane. However, the mass resolving power of the spectrometer is also affected by the time separations between different mass peaks, which is increased by lengthening the drift distance to the detector. Thus, it would seem advantageous to increase the distance to the detector and adjust the voltages applied to the extraction and acceleration regions to place the space-focus plane at the new detector position. Unfortunately, it is found that the minimum achievable width of the ion packet at the space-focus plane increases as its separation from the extraction region is increased, due to the ions' nonzero initial velocity distribution along the direction of the drift path. These conflicting requirements of increased drift length for improved mass temporal separation, and

decreased distance to the space-focus plane for improved isomass pulse width, limit the achievable mass resolving power of a linear TOF mass spectrometer.

With the development and implementation of the "mass-reflectron" [2-4], the above limitation on the TOF mass resolving power was effectively minimized. The operation of the mass-reflectron is schematically illustrated in Figure 1. It is different from the linear TOF mass spectrometer in that it has an electrostatic ion reflector, or mirror, in the drift region, which essentially reverses the direction of the ions and deflects them onto the detector. The operational advantage of this instrument over the linear spectrometer is that it allows the packet compression at the space-focus plane to be positioned near the ion extraction and acceleration regions, and also recreated with good fidelity at the end of the drift region where the detector is located. The physical mechanism by which this is possible is the following. The distribution of the ions at the space-focus plane consists of a minimum spatial extent packet, with a range of velocities (energies) corresponding to the range of initial starting positions in the extraction region, as described above (ignoring the initial velocity distribution for the moment). As this ion packet travels beyond the space-focus plane, the spatial extent grows as the faster ions pull ahead of their slower counterparts. As the packet strikes the ion mirror, the ions of higher energy penetrate more deeply than those of lower energy, causing them an increased time delay in the mirror structure. For a properly formulated electrostatic field distribution in the mirror, the space-focused packet can be recreated with good fidelity at the position of the detector by having the time delay in the mirror precisely compensate for the distribution of flight times outside of the mirror.

A great deal of excellent work has been done incorporating ion mirrors into TOF mass spectrometers, allowing mass resolving powers greatly in excess of that achievable with the original linear geometry [5-7]. It is recognized that in real instruments, determination of the mirror geometry and potentials is problematic due to the difficulty of precisely creating a specified potential distribution in a region of space, as well as the intrinsic three-dimensional nature of the ion packet propagation [8]. However, in many instances, when modeling the performance and optimization of TOF mass spectrometers, a simplified one-dimensional model of the ion mirror is employed and yields useful results.

In the following sections, the exact analytic form of the idealized one-dimensional mirror potential is derived. Previous representations of this potential have been approximate and only piecewise continuous. The relatively simple form for this potential should prove useful in modeling TOF systems, as well as providing a tool in the analysis and design of the more complicated three-dimensional ion mirrors.

## II. Integral equation and solution for mirror potential

### *II.1 Integral Equation derivation*

The idealized one-dimensional problem to be solved is schematically illustrated in Figure 2a. The goal is to find an analytic expression for a "perfect mirror" electrostatic potential such that all ions

(of different velocities, above some threshold) which originate from a plane of perfect spatial focus are brought to a second plane of perfect spatial focus. This requirement is equivalent to specifying that all ions have the same flight-time between the first and second space-focus planes regardless of their initial velocities.

Defining the mirror focal length as $L = L_1 + L_2$, which is the total path length in the field-free regions between the space-focus planes, the total flight time of an ion can be written as

$$T = \frac{L}{v_0} + \delta(v_0) \tag{1}$$

where the first term is the time-of-flight in the field-free region, $\delta(v_0)$ is the time delay in the electrostatic mirror, and $v_0$ is the initial ion velocity. To compute the time delay in the mirror, the equation of conservation of energy of the ion in the mirror potential

$$\frac{1}{2}mv^2(x) + q\Phi(x) = \frac{1}{2}mv_0^2 \tag{2}$$

can be used to solve for $\delta(v_0)$,

$$\delta(v_0) = 2\int_0^t dt' = (2m)^{1/2}\int_0^{X_f} \frac{dx'}{\left(mv_0^2/2 - q\Phi(x')\right)^{1/2}} \tag{3}$$

where $q$ is the ion charge, $\Phi(x)$ is the mirror potential, the factor of 2 in the flight time is to account for the elapsed time entering and exiting the mirror, and $X_f$ is that coordinate for which the mirror potential is equal to the ion incident kinetic energy. This allows Equation (1) to be written in the form of an integral equation for the mirror potential

$$T = \frac{L}{v_0} + (2m)^{1/2}\int_0^{X_f} \frac{dx'}{\left(mv_0^2/2 - q\Phi(x')\right)^{1/2}} \tag{4}$$

where $\Phi(x)$ is chosen such that $T$ is independent of the initial ion velocity, $v_0$.

The solution of this sort of equation under the associated conditions can normally be determined using standard calculus of variations techniques. This involves Laplace transforming the integral equation, using the convolution theorem of Laplace transforms to simplify the integrand, and doing an inverse Laplace transform back to physical variables, which finally leaves an integrable differential equation for the mirror potential. However, the variable to be transformed in this case is the ion initial kinetic energy $mv_0^2/2$, which means that the integral equation must be well-

defined in the limit of zero initial velocity to complete the Laplace transform. Clearly the term representing the time-of-flight in the field-free region, given by $L/v_0$, is singular at this point. This singularity simply originates from the physical fact that an ion with an initial velocity approaching zero has a time-of-flight through the field-free drift region approaching infinity. To resolve this problem, the initial velocity distribution of the ions must be shifted from the velocity distribution of the ions as they enter the mirror potential. This can be easily achieved by placing a short region of uniform retarding electrostatic potential in front of the mirror structure. In this way, only ions with energy above a specified discrimination level reach the mirror. Ions with the minimum energy required to just reach the mirror potential have a finite flight time through the field-free region, and zero velocity as they reach the mirror.

Figure 2b illustrates the mirror structure modified to include the velocity discrimination region (of uniform potential gradient) immediately before the ideal mirror potential region. The integral Equation (4) is modified by the addition of a term reflecting the time-of-flight of an ion through the velocity discrimination region. The uniform potential gradient in this region (generated by a pair of parallel grids held at fixed potential difference) causes a uniform deceleration of the ions, allowing a simple analytic determination of the additional flight time

$$t_d = \frac{2md}{\Delta\phi}\left(v_0 - \sqrt{v_0^2 - \frac{2q\Delta\phi}{m}}\right) \tag{5}$$

where $\Delta\phi$ is the potential drop across the discrimination region, and $d$ is the region length. Furthermore, the expression for the time-delay in the mirror, $\delta(v_0)$, is modified to reflect the decreased kinetic energy of the ions entering the mirror potential. Incorporating these changes yields a new expression for the integral equation describing the ideal mirror potential

$$T = \frac{L}{v_0} + \frac{2md}{\Delta\phi}\left(v_0 - \sqrt{v_0^2 - \frac{2q\Delta\phi}{m}}\right) + (2m)^{1/2}\int_0^{X_f} \frac{dx'}{\left(mv_0^2/2 - q\Delta\phi - q\Phi(x')\right)^{1/2}} \tag{6}$$

*II.2 Reduction to canonical form*

The time-of-flight $T$ in Equation (6) is required to be independent of the initial velocity of the ion. Therefore, its invariant value can be determined from the equation by evaluating the right-hand side for a convenient choice of velocity. For the choice $mv_0^2/2 = q\Delta\phi$ the ion has just enough initial kinetic energy to completely penetrate the velocity discrimination region and arrive at the entrance of the mirror with zero residual velocity. There is no penetration of the mirror fields, which determines the upper limit of the integral in Equation (6) to be zero, and $T$ is simply deter-

mined by the first two terms on the right hand side

$$T \;=\; \frac{L}{\sqrt{2q\Delta\phi/m}} \;+\; \frac{2md}{q\Delta\phi}\,\sqrt{2q\Delta\phi/m}\,. \tag{7}$$

Rewriting all variables in dimensionless form, given by

$$\bar{X} = (X/d) \qquad\qquad \bar{L} \;=\; (L/d)$$

$$\bar{\Phi}\,(\bar{x}) \;=\; \Phi(x)\;/\,\Delta\phi \tag{8}$$

$$\bar{U}_0 \;=\; U_0\;/\;q\Delta\phi$$

where $U_0 \;=\; mv_0^2/2$ , and substituting Equation (7) into the integral Equation (6) yields the simplified expression

$$0 \;=\; \frac{\bar{L}}{2}\left(\frac{1}{\bar{U}_0^{1/2}} - 1\right) \;+\; 2\left(\bar{U}_0^{1/2} - (\bar{U}_0 - 1)^{\,1/2} - 1\right) \;+\; \int_0^{\bar{X}_f} \frac{\mathrm{d}\bar{x}'}{(\bar{U}_0 - 1 - \bar{\Phi}\,(\bar{x}'))^{\,1/2}}. \tag{9}$$

Note that Equation (9) has the expected properties of being clearly satisfied in the limit $\bar{U}_0 \to 1$ , (i.e. as the incident energy approaches the discrimination energy from above), and the expression is independent of the mass, as it must for the mirror to perform properly for all species of ion in the beam.

*II.3 Integral equation solution*

As stated previously, the initial step in obtaining the solution of the integral equation involves performing a Laplace transform. To this end, define the independent variable

$$\xi \;\equiv\; \bar{U}_0 - 1 \;\;=\;\; \bar{\Phi}\,(\bar{X}_f) \tag{10}$$

and the variable of integration

$$\eta \equiv \bar{\Phi}\,(\bar{x}')\;. \tag{11}$$

Equation (11) implies that the integration volume of Equation (9) is transformed by the relation

$$d\eta \;\;=\;\; \left|\frac{d\bar{\Phi}\,(\bar{x}')}{d\bar{x}'}\right| \;\; d\bar{x}'\,. \tag{12}$$

The integral equation then takes the form

$$0 \;=\; \frac{\bar{L}}{2}\left( \frac{1}{(1+\xi)^{1/2}} - 1 \right) \;+\; 2\left( (1+\xi)^{1/2} - \xi^{1/2} - 1 \right) \;+\; \int_0^{\xi} \frac{F(\eta)}{(\xi-\eta)^{1/2}}\, d\eta \qquad (13)$$

where

$$F(\eta) \;=\; \left| \frac{d\bar{\Phi}(\bar{x}')}{d\bar{x}'} \right|^{-1} \qquad (14)$$

is merely the Jacobian factor of the variable transform.

Equation (13) is precisely the same integral equation encountered in a previous work which details the derivation of the form of ideal extraction fields [9], except for the field-free drift distance $\bar{L}$ being replaced by the similar quantity $2\bar{D}$. The generation of the same integral equation for the two problems is not surprising in that both calculations are concerned with deriving a "potential ramp" that either creates or re-creates a space-focus using ions of disparate velocities. The factor of 2 occurs due to the fact that in this calculation the mirror fields are traversed twice during a single ion trajectory.

Using our previous results detailed in [9], the solution to the integral equation can be written down directly as

$$F(\xi) \;=\; \left| \frac{d\bar{\Phi}(\bar{X}_f)}{d\bar{X}_f} \right|^{-1} \;=\; 1 \;-\; \frac{2}{\pi}\mathrm{atan}\left( \bar{\Phi}^{1/2}(\bar{X}_f) \right) \;+\; \frac{\bar{L}}{2\pi} \frac{\bar{\Phi}^{1/2}(\bar{X}_f)}{(1+\bar{\Phi}(\bar{X}_f))}. \qquad (15)$$

From this expression, the variables $\bar{\Phi}$ and $\bar{x}$ can be separated and integrated directly

$$\int_0^{\bar{x}} d\bar{X}_f \;=\; \int_0^{\bar{\Phi}(\bar{x})} \left[ 1 \;-\; \frac{2}{\pi}\mathrm{atan}\left( \bar{\Phi}^{1/2} \right) \;+\; \frac{\bar{L}}{2\pi} \frac{\bar{\Phi}^{1/2}}{(1+\bar{\Phi})} \right] d\bar{\Phi} \qquad (16)$$

yielding

$$\bar{x} \;=\; \frac{(\bar{L}+2)}{\pi}\left( \bar{\Phi}^{1/2}(\bar{x}) \;-\; \mathrm{atan}\left( \bar{\Phi}^{1/2}(\bar{x}) \right) \right) \;+\; \bar{\Phi}(\bar{x}) \left( 1 \;-\; \frac{2}{\pi}\mathrm{atan}\left( \bar{\Phi}^{1/2}(\bar{x}) \right) \right). \qquad (17)$$

This is the desired result of an analytic closed form expression for the ideal one-dimensional mirror potential which recreates a space-focus plane with perfect fidelity.

## III. Discussion and solution verification

The mirror potential of Equation (17) has a simple form in the limit of small $\bar{x}$ and $\bar{\Phi}$, given by

$$\bar{x} \cong \bar{\Phi} + \left(\frac{\bar{L}-4}{3\pi}\right)\bar{\Phi}^{3/2} + \ldots . \tag{18}$$

It is clearly seen to join smoothly to the linear deceleration potential, and for moderate x-positions greater than d, it varies roughly as $x^{2/3}$.

To verify that Equation (17) is the correct analytic expression for the ideal one-dimensional mirror potential, a numerical simulation is performed. For parameter choices of $L = 40$ cm, $d = 0.5$ cm, and $\Delta\phi = 250$ volts, the mirror potential is determined by incrementing $\Phi$ from the starting value of zero, computing $x$ using Equation (17), again incrementing $\Phi$, computing $x$, and iterating until the potential is known over the entire length of the mirror region. The potential computed in this manner is plotted in Figure 3.

Next, for the parameters as specified above, ion trajectories are numerically calculated from the first space-focus plane, through the velocity discrimination region, then in and out of the mirror region, back through the velocity discrimination fields, and on to the second space-focus plane. This is done for a range of initial ion energies from 251 eV to 2000 eV, and the results are plotted in Figure 4. The desired properties are strikingly confirmed as it is observed that the time delay in the mirror exactly compensates for the different field-free drift times of the ions of different initial velocities, yielding a total flight time independent of initial velocity. This is precisely the behavior required of an ideal ion mirror, which recreates an image of an initial space-focus plane with perfect fidelity.

## IV. Conclusions

It has been demonstrated that an analytic closed-form solution exists for the potential distribution of an ideal one-dimensional electrostatic ion mirror. The functional form is very similar to that previously derived for the ideal non-linear extraction fields [9], as one would expect from physical analogies. This result can be useful in designing and analyzing realistic three-dimensional ion mirrors, and the potential performance characteristics of TOF instruments employing these devices.

## References

[1] W.C. Wiley and I.H. McLaren, Rev. Sci. Instrum., 26 (1955) 1150.

[2] V.I. Karataev, B.A. Mamyrin, and D.V. Shmikk, Sov. Phys. JETP 16 (1972) 1177.

[3] B.A. Mamyrin, V.I. Karataev, D.V. Shmikk, and V.A. Zagulin, Sov. Phys. JETP 37 (1973) 45.

[4] B.A. Mamyrin and D.V. Shmikk, Sov. Phys. JETP 49 (1979) 762.

[5] W. Gohl, R. Kutscher, H.J. Laue, and H. Wollnik, Int. J. Mass Spectrom. Ion Phys., 48 (1983) 411.

[6] H. Danigel, H. Jungclas, and L. Schmidt, Int. J. Mass Spectrom. Ion Phys., 52 (1983) 223.

[7] R. Grix, R. Kutscher, G. Li, U. Gruner, and H. Wollnik, Rapid Commun. Mass Spectrom., 2 (1988) 83.

[8] R. Kutscher, R. Grix, G. Li, and H. Wollnik, Int. J. Mass Spectrom. Ion Processes., 103 (1991) 117.

[9] C.A. Flory, R.C. Taber, and G.E. Yefchak, submitted to Int. J. Mass Spectrom. Ion Processes. (1995).

## Figure Captions

Fig. 1. Schematic illustration of a TOF mass spectrometer incorporating an electrostatic ion mirror to recreate the space-focus at the position of the detector.

Fig. 2a. Idealized representation of the one-dimensional ion mirror. The arrows represent the initial velocities of the individual ions.

Fig. 2b. The one-dimensional ion mirror modified to include a velocity discrimination region of uniform potential gradient in front of the non-linear mirror fields.

Fig. 3. The ideal one-dimensional non-linear mirror fields computed from Equation (17) for $L = 40$ cm, $d = 0.5$ cm, and $\Delta\phi = 250$ volts.

Fig. 4. Computed ion flight times for the portions of the trajectories inside and outside the non-linear mirror fields, as well as the total flight times. The ions have energies ranging from 251 eV to 2000 eV, the mass is 100 u, and the other parameters are the same as in Figure 3.

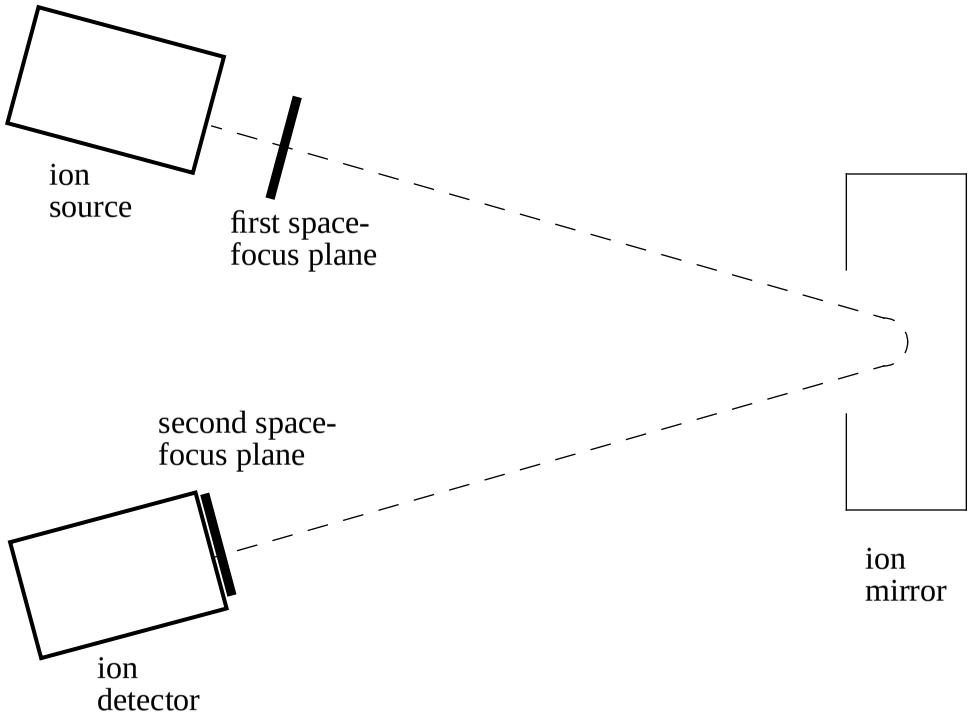
ion
source
first space-
focus plane
second space-
focus plane
ion
mirror
ion
detector

Figure 1

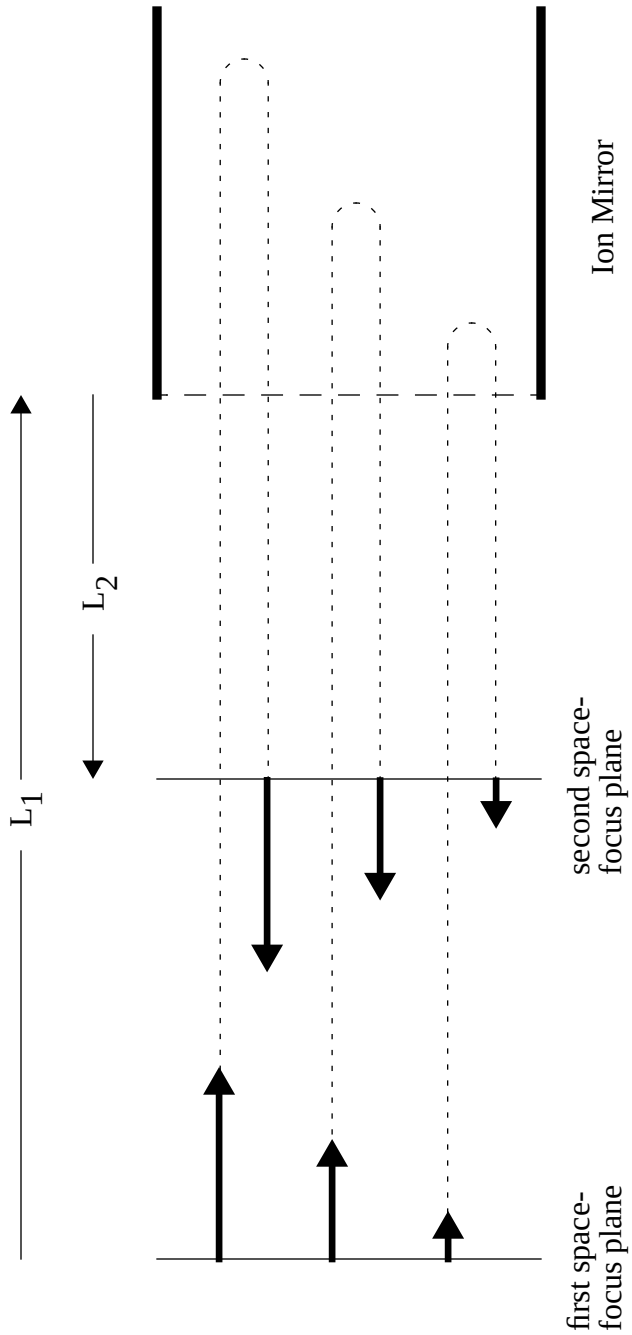
Ion Mirror
second space-focus plane
first space-focus plane
L1
L2

Figure 2a

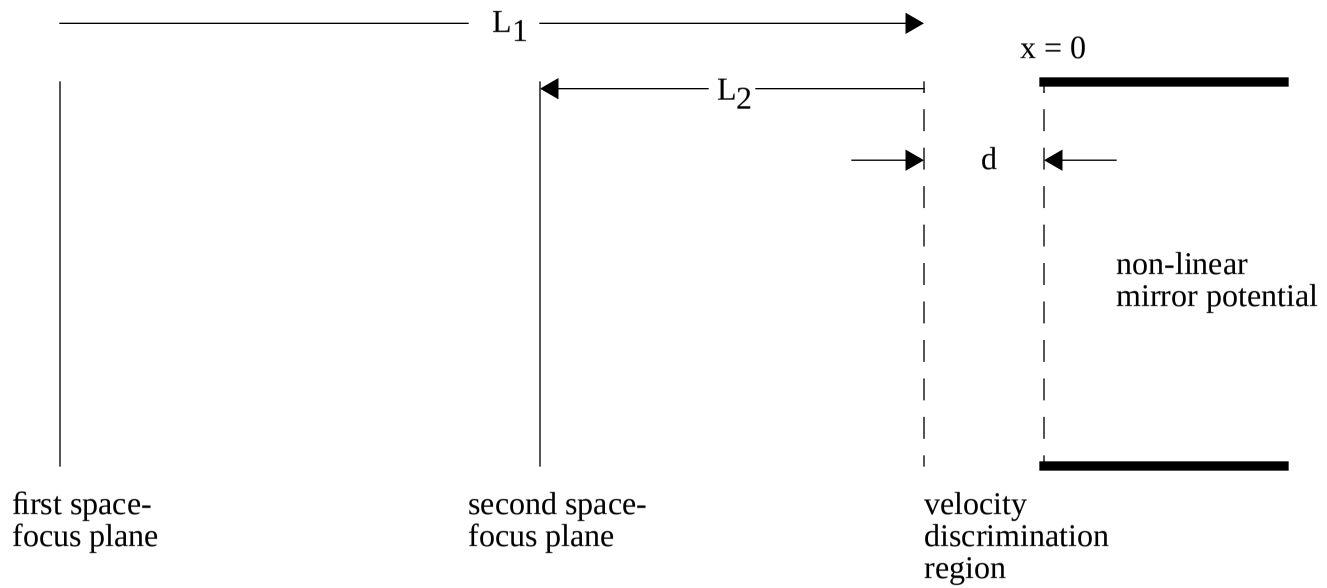
L1
x = 0
L2
d
non-linear
mirror potential
first space-
focus plane
second space-
focus plane
velocity
discrimination
region

Figure 2b

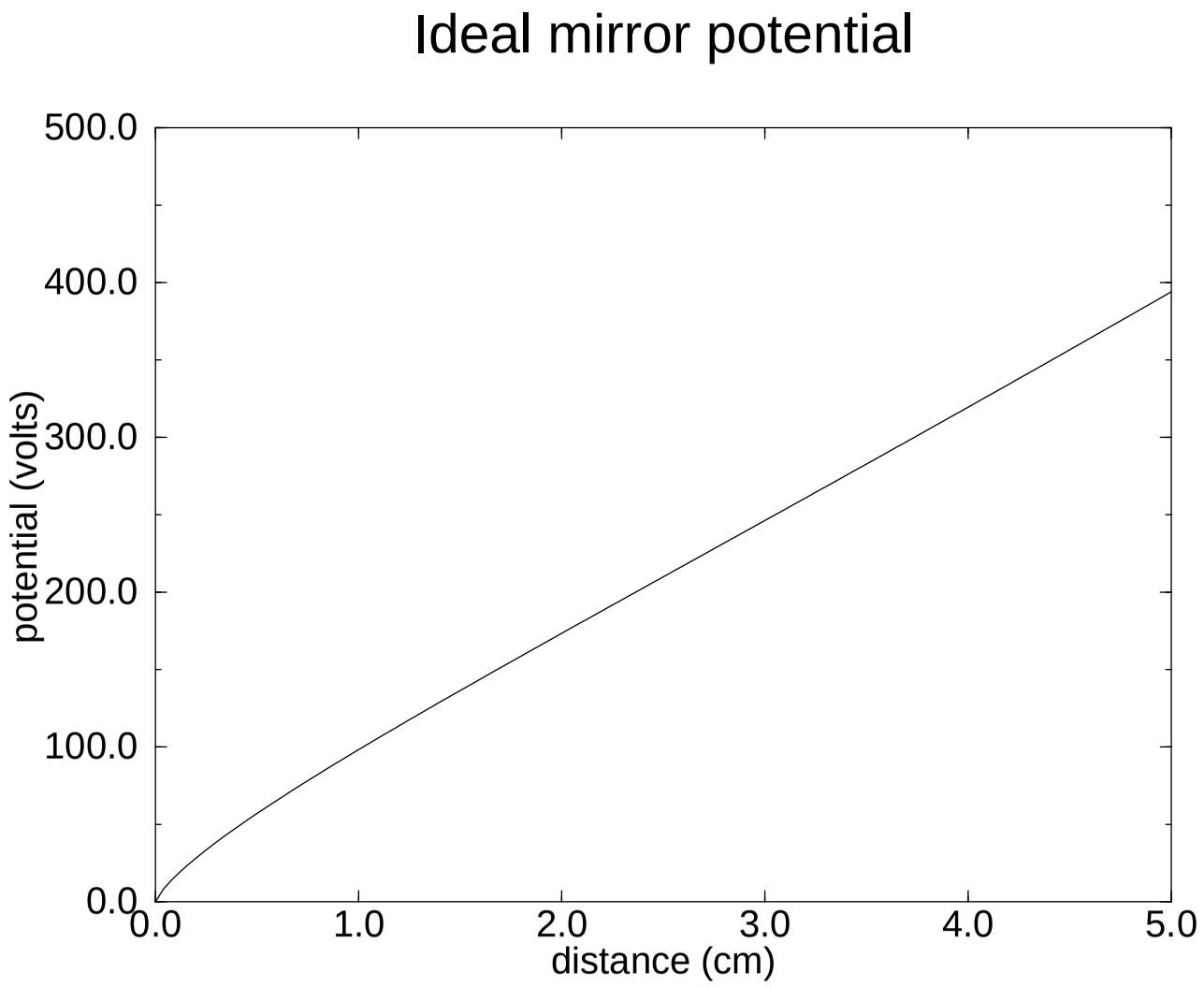
Ideal mirror potential
500.0
400.0
300.0
200.0
100.0
0.0
potential (volts)
0.0
1.0
2.0
3.0
4.0
5.0
distance (cm)

Figure 3

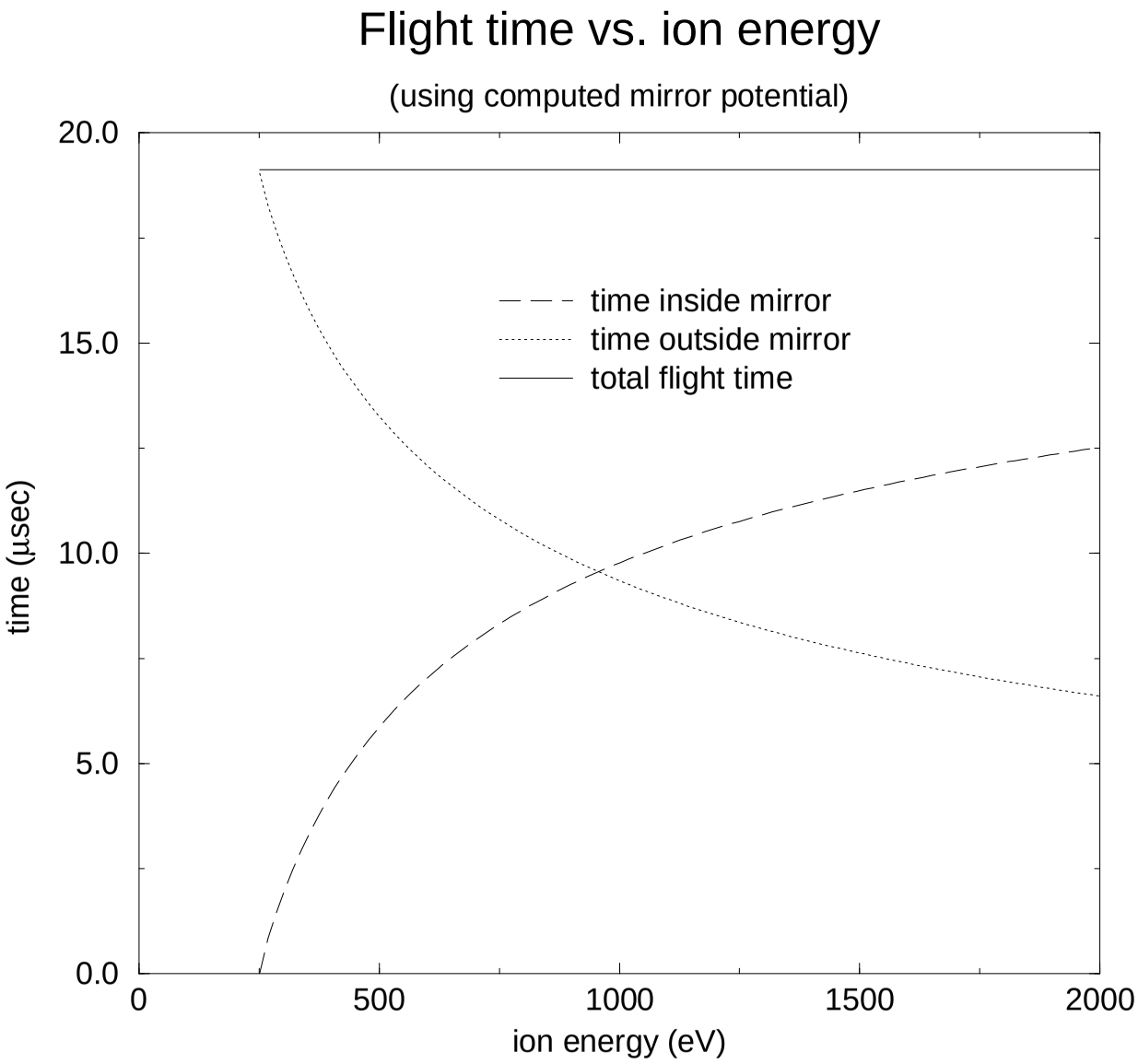
Flight time vs. ion energy
(using computed mirror potential)
time inside mirror
time outside mirror
total flight time
time (µsec)
ion energy (eV)
20.0
15.0
10.0
5.0
0.0
0
500
1000
1500
2000

Figure 4